ChemComm

COMMUNICATION

View Article Online
View Journal | View Issue

Open Access Article. Published on 22 July 2015. Downloaded on 12/4/2025 6:44:22 PM.
This article is licensed under a Creative Commons Attribution-NonCommercial 3.0 Unported Licence.

Cite this: *Chem. Commun.*, 2015, **51**, 13850

Received 22nd May 2015,
Accepted 22nd July 2015

DOI: 10.1039/c5cc04234h

www.rsc.org/chemcomm

Pulsed EPR spectroscopy distance measurements of DNA internally labelled with Gd^{3+}-DOTA†

Filip Wojciechowski,[a] Andreas Groß,[ab] Isabelle T. Holder,[ab] Laura Knörr,[a] Malte Drescher*[ab] and Jörg S. Hartig*[ab]

Gd^{3+} is increasingly used in EPR spectroscopy due to its increased intracellular stability and signal-to-noise ratios. Here we present the incorporation of Gd^{3+}-DOTA into internal positions in DNA. Distance measurements *via* pulsed Electron Paramagnetic Resonance (EPR) spectroscopy *in vitro* and *in cellula* proved enhanced stability and efficiency compared to nitroxide labels.

Pulsed electron paramagnetic resonance (EPR) spectroscopy has emerged as a powerful technique in the study of the molecular structure and dynamics of biomacromolecules under *in vitro* conditions[1–3] as well as in the cellular milieu.[4–10] The pulsed EPR method double electron–electron resonance (DEER) in combination with site-directed labelling (SDSL) of biomacromolecules facilitates distance measurements between two spin labels in the nanometer range.[11–13] Typically, a paramagnetic label based on a stable nitroxide radical with the general structural building block of RNO• is used as a spin label. However, alternative paramagnetic compounds are being investigated for their use as EPR probes in biomacromolecules.

Within the context of oligonucleotides (DNA, RNA and non-canonical oligonucleotide structures) EPR spectroscopy has been proven to be extremely useful for measuring distance distributions and studying conformational changes in polymorphic non-canonical DNA structures called G-quadruplexes, which were labelled with SDSL.[14–16] Similarly, EPR has been used to detect the formation of both duplex and triplex DNA structures.[17] Recently, X-band continuous wave-EPR spectroscopy has been applied to detect abasic sites in duplex DNA as well as in base-pair mismatch detection.[18]

However, while nitroxide radicals have been extensively used in EPR spectroscopy *in vitro*, they have some drawbacks in the context of high field EPR measurements *in cellula*. When used in cell studies, the nitroxide radicals encounter the reducing environment of the cellular milieu which can quench the nitroxide to an EPR-silent *N*-hydroxyl derivative.[6,7] To overcome this limitation and benefit from further advantages, especially gadolinium-based spin labels become more and more the focus of attention and were used in several approaches for pulsed EPR distance measurements.[19–23] The lanthanide gadolinium in the oxidation state of 3+ has recently been used as a paramagnetic centre in in-cell EPR spectroscopy.[9,10] Besides the stability of these spin labels inside the cellular milieu, they furthermore excel by no orientation selection, higher transition moments owing to the high spin system of $S = 7/2$, fast repetition rates due to the short longitudinal relaxation (T_1) rates and therefore increased signal-to-noise-ratios of DEER experiments in comparison to standard nitroxide labels.[19]

The macrocycle 1,4,7,10-tetraazacyclododecane-1,4,7,10-tetraacetic acid (DOTA) has been extensively used to chelate Gd^{3+}.[24–26] DOTA is one of the most powerful metal chelating agents for lanthanide ions[27] and is used as a contrast agent in magnetic resonance imaging in the medical diagnosis.[28,29] Recently Gd^{3+}-DOTA has been attached by SDSL at the 5′-position of oligonucleotides using click chemistry and was used in model EPR distance measurements.[30] However, future applications of Gd^{3+}–Gd^{3+} DEER distance measurements in oligonucleotides would benefit from being able to internally label oligonucleotides at any desired position with Gd^{3+}-DOTA. This would allow for studying a much broader range of nucleic acid structures *via* Gd^{3+}–Gd^{3+} DEER measurements.

There are two main strategies for the internal labelling of oligonucleotides with Gd^{3+}-DOTA; addition of a Gd^{3+}-DOTA phosphoramidite during solid-phase synthesis or post-synthetic labelling either in solution or on the solid-phase resin. The synthesis of a DOTA phosphoramidite has been described.[31] However, the DOTA unit was appended at the N3 position of uracil, thereby preventing the modified nucleobase to undergo Watson–Crick base-pairing and limiting its incorporation to the ends of oligonucleotides where it has a minimal destabilizing effect.

[a] *Department of Chemistry, University of Konstanz, Universitätsstr. 10, Konstanz, Germany. E-mail: joerg.hartig@uni-konstanz.de, malte.drescher@uni-konstanz.de; Tel: +49-7531884575*

[b] *Konstanz Research School Chemical Biology, University of Konstanz, Germany*

† Electronic supplementary information (ESI) available: Experimental details and additional experiments. See DOI: 10.1039/c5cc04234h

This journal is © The Royal Society of Chemistry 2015

Open Access Article. Published on 22 July 2015. Downloaded on 12/4/2025 6:44:22 PM.
This article is licensed under a Creative Commons Attribution-NonCommercial 3.0 Unported Licence.

Furthermore, due to the likely incompatibility of metalated DOTA (*e.g.* Gd^{3+}-DOTA) in solid-phase oligonucleotide synthesis the metal needs to be introduced post-synthetically.

Therefore we have decided to pursue a post-synthetic labelling strategy on the solid-phase resin using copper-catalysed 1,3-dipolar cycloaddition reaction (click chemistry).[32,33] There are many examples of click chemistry between alkyne modified oligonucleotides and azides.[34] However the synthesis of azide labelled oligonucleotides is less common.[35] This is due to the instability of azides to P(III) oligonucleotide chemistry: the azide undergoes Staudinger reaction during oligonucleotide synthesis.[36]

Herein, we describe the synthesis of a phosphoramidite building block that was used in the automated DNA synthesis of azides containing DNA, which was subsequently reacted with alkyne-(Gd^{3+}-DOTA)[37,38] to give internally labelled (Gd^{3+}-DOTA)-DNA. We characterize a DNA duplex with respect to the influence of the Gd-DOTA label on the stability and structure of the dsDNA helix. Then, we performed EPR spectroscopy-based distance measurements of these modified oligonucleotides both *in vitro* and *in cellula.*

The C5 position of uracil was chosen to attach Gd^{3+}-DOTA to DNA. Bulky substituents can be incorporated at this position without influencing the *syn*/*anti* equilibrium around the glycosidic bond and therefore minimally perturbing the duplex DNA structure. A variety of tethers and tether lengths were considered to attach Gd^{3+}-DOTA to the C5 position of uracil. However, as a proof of principle we reasoned that 5-hexyn-1-ol should be long enough to allow for on-resin post-synthetic click chemistry with alkyne Gd^{3+}-DOTA. Shorter length linkers such as 3-butyn-1-ol could have placed the alkyl-azide in a sterically hindered environment thus inhibiting the click chemistry reaction.[39] Conversely, a longer tether might result in a larger distance distribution in DEER-EPR due to residual motion of the Gd^{3+}-DOTA. The synthesis of phosphoramidite **2** begins with 5′-DMT-5-iodo-2′-deoxyuridine (DMT-5-I-dU)[40] and is accomplished in three steps (Scheme 1). Sonogashira cross-coupling[41] between DMT-5-I-dU and 5-hexyn-1-ol gave **1** in 72%. Conversion of the hydroxyl group to the iodo group proceeded without difficulty using $(PhO)_3PCH_3I$ in DMF, followed by phosphitylation using standard conditions to give the phosphoramidite building block **2** in 52% over two steps.

Kool and co-workers have described that an iodothymidine phosphoramidite is stable towards standard automated DNA synthesis conditions.[42] Furthermore, the iodo group may be easily displaced by various nucleophiles such as sodium azide.[43,44] Based on these results, we reasoned that the iodo-containing phosphoramidite **2** would be compatible with DNA synthesis conditions and provide access to azide containing DNA.

Two modified oligodeoxynucleotides were synthesized DNA 1 5′-GCGAGTGACTGGTATGA**X**GATGCT-3′ and DNA 2 5′-AGCATC ATCATACCAG**X**CACTCGC-3′ containing the modified building block **X** (Scheme 2). The iodo-containing resin-bound DNAs (DNA 1 or DNA 2) were converted to the corresponding azides using an excess of NaN_3 at 50 °C. Alkyne-(Gd^{3+}-DOTA) was prepared as described by M.G Finn and co-workers.[37] On-resin click chemistry between the azide DNAs and alkyne-(Gd^{3+}-DOTA) gave the desired Gd^{3+}-DOTA containing DNAs, for details see the ESI.† The modified DNAs were deprotected under standard ammonia conditions followed by RP-HPLC purification, and characterization by ESI-MS. The purity was controlled *via* PAGE analysis and the labelling efficiency was calculated to be 80% *via* cw EPR.

Duplex DNA (DNA 1/DNA 2) resulted in a decrease in thermal stability ($\Delta T_m = -10$ °C, $T_m = 54$ °C) and a deviation from a two-state melting profile when compared to the duplex control sequence ($T_m = 64$ °C), Fig. 1a. Next we performed CD spectroscopy in order to gain insight into the structure of the

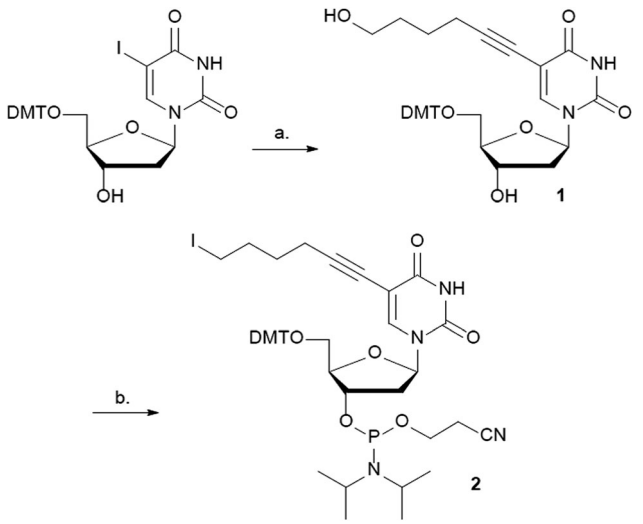

Scheme 1 Synthesis of phosphoramidite **2**. *Reagents and conditions*: (a) $Pd(PPh_3)_2Cl_2$, CuI, NEt_3, 5-hexyn-1-ol, THF, rt, 16 h, 72%; (b) (i) $(PhO)_3P$-CH_3I, DIPEA, DMF, rt, 6 h, (ii) Cl-(i-Pr)$_2$NPOCH$_2$CH$_2$CN, DIPEA, CH_2Cl_2, rt, 2 h, 52% (2 steps).

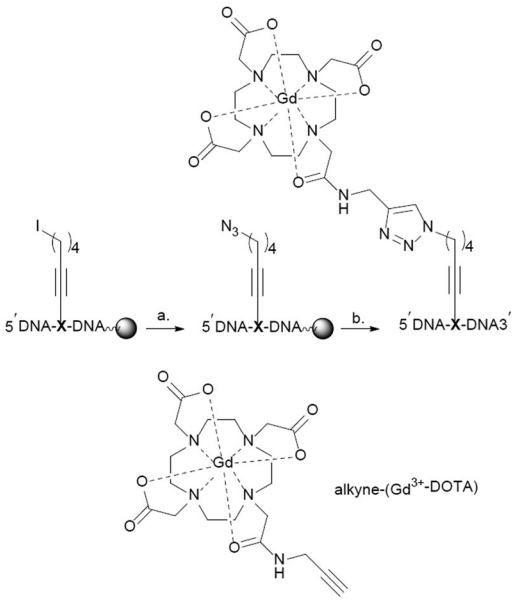

Scheme 2 On-resin synthesis of internally labelled DNA. (a) NaN_3, DMF, 55 °C. 24 h; (b) (i) TBTA, sodium ascorbate, $CuSO_4$, alkyne-(Gd^{3+}-DOTA), DMF/H_2O, 50 °C, (ii) NH_4OH, 50 °C, 12 h. X represents the modified nucleotide containing building block **2**.

Open Access Article. Published on 22 July 2015. Downloaded on 12/4/2025 6:44:22 PM.
This article is licensed under a Creative Commons Attribution-NonCommercial 3.0 Unported Licence.

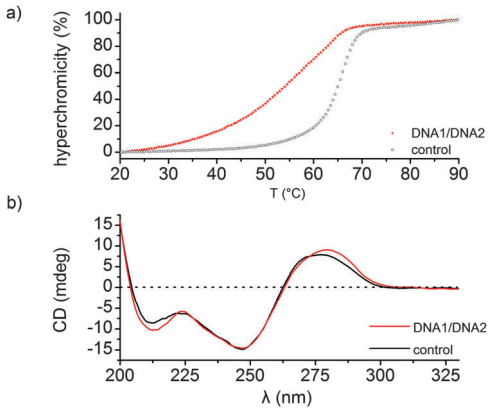

Fig. 1 Thermal denaturation and CD spectra. (a) UV-thermal denaturation curve of the modified duplex DNA (DNA 1/DNA 2, T_m = 54 °C) and the control sequence (T_m = 64 °C). (b) CD spectra of duplex DNA 1/DNA 2 and the control sequence.

DNA duplex. A typical B-type conformation with almost equal positive (275 nm) and negative (245 nm) ellipticity zeroing at 260 nm was observed (Fig. 1b). Altogether attaching the Gd-DOTA to DNA has a destabilizing effect when compared to the unmodified DNA as observed by a decrease in thermal stability. However CD spectroscopy indicates that the modified duplex exists as a B-DNA duplex.

Q-Band (34 GHz) EPR-experiments of the internally labelled duplex DNA were carried out in deuterated Tris-HCl buffer and inside *Xenopus laevis* oocytes (for in-cell samples see Fig. 2a). The oocytes for these samples were shock-frozen after 15 minutes of incubation time. Although Gd^{3+}-complexes are stable in the cellular milieu for hours,[9,10] we noticed a cytotoxic effect of the Gd^{3+} labelled duplex DNA for the oocytes. We observed the disruption of the vitelline membrane of the oocytes after 1 hour of incubation after microinjection. Even after 15 min of incubation signs of apoptosis were observable as loss of pigment in the animal pole. However, the vitelline membrane was still intact and no leakage was observed (see the ESI† for details). The central transition-normalized echo-detected field sweeps of

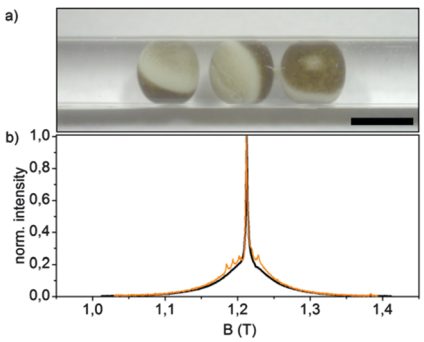

Fig. 2 (a) Micrograph of a DEER-sample of 3 oocytes of *Xenopus laevis* in a Q-band test tube after 15 min incubation at 18 °C with 50 nL of 3.7 mM duplex DNA microinjected in each oocyte, scale bar = 1 mm; (b) normalized Q-band two-pulse echo-detected field sweeps of duplex DNA in buffer (black) and inside *Xenopus laevis* oocytes after 15 min incubation (orange), measured after shock-freezing at 10 K.

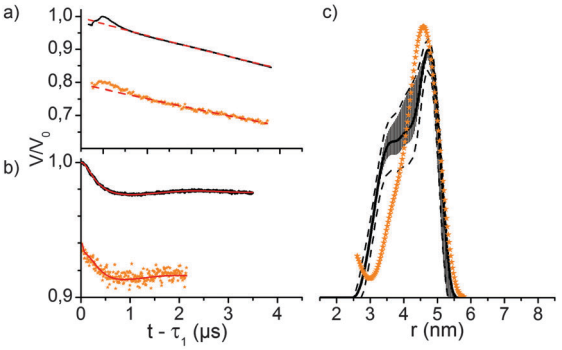

Fig. 3 (a) Four-pulse DEER traces of duplex DNA in buffer (black) and inside *Xenopus laevis* oocytes after 15 min incubation (orange) recorded at the Q-band (T = 10 K) and corresponding background fits (dashed red lines), assuming a homogeneous 3D distribution of molecules; (b) background-corrected DEER form factor of the corresponding experiments with Tikhonov regularization fit (red); (c) distance distribution obtained from Tikhonov regularization of the corresponding measurements; observer pulses 14/14/28 ns, pump pulses 16 ns (buffer), 18 ns (in-cell), $\Delta\nu$ = 125 MHz, accumulation time 17 h (buffer) or 20 h (in-cell); (c) distance distributions obtained *via* Tikhonov regularization of the corresponding DEER traces of dsDNA in buffer (black) and inside *Xenopus laevis* oocytes (orange). The error bars are the full variation of the probability of the given distance distribution (black) obtained during the statistical analysis, whereas the dotted lines are upper/lower error estimations corresponding to the mean value +/− two times the standard deviation of the different Tikhonov fits.

the *in vitro* (black) and intracellular (orange) samples are shown in Fig. 3b. The spectral shape of both experiments are similar, whereas the intracellular measurement features a further superimposed sextet signal allocated to endogenous Mn^{2+} species.[9,10]

Q-band-DEER-measurements of the internally labelled duplex DNA (100 μM) were carried out in deuterated Tris-HCl buffer (pH = 7.4) at T = 10 K. The label efficiency was calculated to be 80% by determination of spin concentration *via* EPR (echo-detected field sweep shown in Fig. 2b). Fig. 3a shows the DEER-curve (black) with 3-dimensional background function (red) and Fig. 3b shows the background corrected form factor (black) with model-free Tikhonov-regularization fit (red), respectively. The modulation depth λ = 2% is expected for DOTA-based labels under the applied conditions.[20] The received distance distribution of the *in vitro* experiment is shown in Fig. 3c (black), featuring a mean distance of 4.8 nm. However, validation of these data *via* 160 Tikhonov-regularizations (shown as error bars as described in the Experimental section) reveals that the shoulder at 3.8 nm should not be over-interpreted. In spite of the rather long tether of the spin label, we find a distance distribution featuring a half width at half maximum of 0.83 nm, which is slightly broader as reported by Song *et al.* for a terminally Gd(III) labelled DNA.[23]

For EPR distance measurements of the duplex DNA inside *Xenopus laevis* 50 nL stock solution (3.7 mM DNA in Tris-HCl buffer) were microinjected into each cell. The average spin concentration in the sample determined by the echo-detected field sweep is 180 μM with a local concentration of 350 μM as calculated from the dipolar evolution curve. The corresponding

Open Access Article. Published on 22 July 2015. Downloaded on 12/4/2025 6:44:22 PM.
This article is licensed under a Creative Commons Attribution-NonCommercial 3.0 Unported Licence.

DEER-curve and form factor are shown in Fig. 3a and b in orange. The modulation depth of the form factor is comparable with the modulation depth of the *in vitro* measurement, but the signal-to-noise is worse since the transverse relaxation time of T_2 = 1.4 ms is significantly shorter than the transverse relaxation time of the *in vitro* measurement with T_2 = 4.0 ms (see Fig. S2, ESI†). Furthermore, the signal-to-noise ratio of the DEER form factor is reduced by the endogenous, spatially 3-dimensionally distributed Mn^{2+} species which contributes solely to the measurement background, effectively reducing the signal-to-noise ratio.[9] The distance distribution *in cellula* obtained by Tikhonov-regularization is shown in Fig. 3c. Due to the short dipolar evolution time of the measurement solely the mean distance of the distance distribution is reliable and the discussion of shape and width would involve the over-interpretation of the available experimental data. Still, the obtained mean distance fits quite well with the mean distance of the measurement in buffer, displaying the stability of the doubly internally labelled duplex DNA and of the label itself.

In conclusion we have introduced a straightforward method for labelling oligonucleotides internally with Gd^{3+}-labels. The formerly utilized 5′-end could in principle be utilized for additional modifications. More importantly, internal labels give more flexibility in terms of the investigated structures. For example, individual domains or parts within the context of larger nucleic acid sequences can be characterized by internal labelling strategies. Although the stability of the investigated duplex DNA decreased, importantly the observed B-DNA structure was not disturbed. Moreover, the internal Gd labels allowed measurement of intermolecular distances of the labelled DNA duplex. An increasing field of interest is the application of EPR spectroscopy in cellular environments. For this purpose, modified biomolecules are introduced into cells and EPR measurements are carried out. Here, we demonstrate the utilization of internal Gd labels for acquiring distance measurements in *Xenopus* oocytes. Compared to nitroxide labels utilized so far, Gd labels have the advantage of increased intracellular stability. However, we observed pronounced cytotoxicity of the Gd-labelled DNAs that might prohibit investigations over extended times.

Notes and references

1 G. Jeschke, *Annu. Rev. Phys. Chem.*, 2012, **63**, 419–446.
2 Y. Shin, C. Levinthal, F. Levinthal and W. Hubbell, *Science*, 1993, **259**, 960–963.
3 D. T. Yu, A. D. Milov and A. G. Maryasov, *Russ. Chem. Rev.*, 2008, **77**, 487.
4 M. Azarkh, V. Singh, O. Okle, I. T. Seemann, D. R. Dietrich, J. S. Hartig and M. Drescher, *Nat. Protoc.*, 2013, **8**, 131–147.
5 M. Azarkh, O. Okle, V. Singh, I. T. Seemann, J. S. Hartig, D. R. Dietrich and M. Drescher, *ChemBioChem*, 2011, **12**, 1992–1995.
6 M. Azarkh, O. Okle, P. Eyring, D. R. Dietrich and M. Drescher, *J. Magn. Reson.*, 2011, **212**, 450–454.
7 I. Krstić, R. Hänsel, O. Romainczyk, J. W. Engels, V. Dötsch and T. F. Prisner, *Angew. Chem., Int. Ed.*, 2011, **50**, 5070–5074.
8 R. Igarashi, T. Sakai, H. Hara, T. Tenno, T. Tanaka, H. Tochio and M. Shirakawa, *J. Am. Chem. Soc.*, 2010, **132**, 8228–8229.
9 M. Qi, A. Groß, G. Jeschke, A. Godt and M. Drescher, *J. Am. Chem. Soc.*, 2014, **136**, 15366–15378.
10 A. Martorana, G. Bellapadrona, A. Feintuch, E. Di Gregorio, S. Aime and D. Goldfarb, *J. Am. Chem. Soc.*, 2014, **136**, 13458–13465.
11 M. Pannier, S. Veit, A. Godt, G. Jeschke and H. W. Spiess, *J. Magn. Reson.*, 2000, **142**, 331–340.
12 A. D. Milov, A. G. Maryasov and Y. D. Tsvetkov, *Appl. Magn. Reson.*, 1998, **15**, 107–143.
13 J. E. Banham, C. M. Baker, S. Ceola, I. J. Day, G. H. Grant, E. J. J. Groenen, C. T. Rodgers, G. Jeschke and C. R. Timmel, *J. Magn. Reson.*, 2008, **191**, 202–218.
14 V. Singh, M. Azarkh, T. E. Exner, J. S. Hartig and M. Drescher, *Angew. Chem., Int. Ed.*, 2009, **48**, 9728–9730.
15 I. T. Holder, M. Drescher and J. S. Hartig, *Bioorg. Med. Chem.*, 2013, **21**, 6156–6161.
16 C. Rehm, I. T. Holder, A. Groß, F. Wojciechowski, M. Urban, M. Sinn, M. Drescher and J. S. Hartig, *Chem. Sci.*, 2014, **5**, 2809–2818.
17 P. M. Gannett, E. Darian, J. Powell, E. M. Johnson, C. Mundoma, N. L. Greenbaum, C. M. Ramsey, N. S. Dalal and D. E. Budil, *Nucleic Acids Res.*, 2002, **30**, 5328–5337.
18 U. Jakobsen, S. A. Shelke, S. Vogel and S. T. Sigurdsson, *J. Am. Chem. Soc.*, 2010, **132**, 10424–10428.
19 D. Goldfarb, *Phys. Chem. Chem. Phys.*, 2014, **16**, 9685–9699.
20 A. M. Raitsimring, C. Gunanathan, A. Potapov, I. Efremenko, J. M. L. Martin, D. Milstein and D. Goldfarb, *J. Am. Chem. Soc.*, 2007, **129**, 14138–14139.
21 H. Yagi, D. Banerjee, B. Graham, T. Huber, D. Goldfarb and G. Otting, *J. Am. Chem. Soc.*, 2011, **133**, 10418–10421.
22 P. Lueders, H. Jäger, M. A. Hemminga, G. Jeschke and M. Yulikov, *J. Phys. Chem. B*, 2013, **117**, 2061–2068.
23 Y. Song, T. J. Meade, A. V. Astashkin, E. L. Klein, J. H. Enemark and A. Raitsimring, *J. Magn. Reson.*, 2011, **210**, 59–68.
24 M. Bottrill, L. Kwok and N. J. Long, *Chem. Soc. Rev.*, 2006, **35**, 557–571.
25 G. J. Stasiuk and N. J. Long, *Chem. Commun.*, 2013, **49**, 2732–2746.
26 T. P. Gazzi, L. A. Basso, D. S. Santos and P. Machado, *RSC Adv.*, 2014, **4**, 9880–9884.
27 L. Lattuada, A. Barge, G. Cravotto, G. B. Giovenzana and L. Tei, *Chem. Soc. Rev.*, 2011, **40**, 3019–3049.
28 N. Viola-Villegas and R. P. Doyle, *Coord. Chem. Rev.*, 2009, **253**, 1906–1925.
29 P. A. Bonnet, A. Michel, J. P. Fernandez, C. Cyteval, A. Rifai, M. Boucard, J. P. Chapat and J. L. Lamarque, *Magn. Reson. Imaging*, 1990, **8**, 71–77.
30 Y. Song, T. J. Meade, A. V. Astashkin, E. L. Klein, J. H. Enemark and A. Raitsimring, *J. Magn. Reson.*, 2011, **210**, 59–68.
31 J. Hovinen, *Nucleosides, Nucleotides Nucleic Acids*, 2007, **26**, 1459–1462.
32 V. V. Rostovtsev, L. G. Green, V. V. Fokin and K. B. Sharpless, *Angew. Chem., Int. Ed.*, 2002, **41**, 2596–2599.
33 C. W. Tornøe, C. Christensen and M. Meldal, *J. Org. Chem.*, 2002, **67**, 3057–3064.
34 A. H. El-Sagheer and T. Brown, *Chem. Soc. Rev.*, 2010, **39**, 1388–1405.
35 M. Gerowska, L. Hall, J. Richardson, M. Shelbourne and T. Brown, *Tetrahedron*, 2012, **68**, 857–864.
36 T. Wada, A. Mochizuki, S. Higashiya, H. Tsuruoka, S. Kawahara, M. Ishikawa and M. Sekine, *Tetrahedron Lett.*, 2001, **42**, 9215–9219.
37 J. D. E. Prasuhn, R. M. Yeh, A. Obenaus, M. Manchester and M. G. Finn, *Chem. Commun.*, 2007, 1269–1271.
38 R. F. H. Viguier and A. N. Hulme, *J. Am. Chem. Soc.*, 2006, **128**, 11370–11371.
39 J. Gierlich, G. A. Burley, P. M. E. Gramlich, D. M. Hammond and T. Carell, *Org. Lett.*, 2006, **8**, 3639–3642.
40 R. H. E. Hudson and A. Ghorbani-Choghamarani, *Synlett*, 2007, 0870–0873.
41 K. Sonogashira, *J. Organomet. Chem.*, 2002, **653**, 46–49.
42 Y. Xu and E. T. Kool, *Tetrahedron Lett.*, 1997, **38**, 5595–5598.
43 G. P. Miller and E. T. Kool, *J. Org. Chem.*, 2004, **69**, 2404–2410.
44 G. P. Miller and E. T. Kool, *Org. Lett.*, 2002, **4**, 3599–3601.